Talanta 125 (2014) 107–113

Contents lists available at ScienceDirect

Talanta

journal homepage: www.elsevier.com/locate/talanta

Fluorescence detection for phosphate monitoring using reverse injection analysis

Lars Kröckel*, Hartmut Lehmann, Torsten Wieduwilt, Markus A. Schmidt

Leibniz Institute of Photonic Technology (IPHT Jena), Albert-Einstein-Str. 9, 07745 Jena, Germany

ARTICLE INFO

Article history:
Received 13 December 2013
Received in revised form
21 February 2014
Accepted 27 February 2014
Available online 5 March 2014

Keywords:
Fluorescence
Detector
Sensor
Flow injection analysis
Phosphate

ABSTRACT

We present a novel design for a compact flow-through fluorescence detector for flow analyses applications and prove its functionality in the experiment. The detector operates by detecting the diffusely emitted fluorescence in a glass capillary, which is a measure for the concentration of the analyte to be detected. The fluorescence is excited via an axially coupled fibre providing LED light and is collected by a photodiode. As model analyte we used dissolved reactive phosphate. The determination of the phosphate concentration is based on the reaction of molybdate to phosphomolybdate, which quenches the fluorescence of Rhodamine 6G. The experiments rely on a reversed flow injection analysis system especially designed for decoupling the analytical setup from environmental pressure for in situ applications. By combining the optics part and the fluidic setup a measuring range of 0–40 $\mu g\,L^{-1}$ PO_4–P with detection limits of 0.22 $\mu g\,L^{-1}$ PO_4–P (7 nmol L^{-1}) for water and of 0.45 $\mu g\,L^{-1}$ PO_4–P (14.5 nmol L^{-1}) for seawater have been obtained. Our novel system has a sampling frequency of up to 300 samples per hour and achieves a repeatability between 0.6% (RSD) for the blank value signal ($n=15$) and 4.6% (RSD) for a phosphate concentration of 20.8 $\mu g\,L^{-1}$ PO_4–P ($n=15$).

1. Introduction

Monitoring and analysing water quality is a key to several important applications: *water* is nutrition base for life (drinking water), is used for different types of processing (e.g. ultrapure water in semiconductor technologies), is recycled from waste water, and is a natural habitat for a variety of wildlife. These different kinds of water have to be controlled according to different regulations. The monitoring process requires data collection, data evaluation, and the formulation of adequate management reactions to improve the environment status or address separate problems. This approach to solving such problems fails if the data collected are incorrect due to unqualified analytical methods or inappropriate sampling, transport, and storage protocols [1].

Several flow analysis techniques have been developed in recent decades for producing large data sets of spatial distributions or temporal trends of investigated water compounds [2,3]. Mapping or in situ monitoring applications place a high demand on the instrumentation towards good accuracy, precision, selectivity, and sensitivity. The systems should be robust, portable, reliable, fast, have miniaturised components, and consume low levels of reagents and energy. In the last sixty years the concentrations of nutrients have been increasing significantly due to intensified agriculture, industry, and traffic [4]. High levels of nutrients lead to a drastic increase in algae growth and, eventually, to eutrophication. Therefore, continuous monitoring of nutrients in natural waters is necessary to ensure water quality [5]. The increasing need for water quality monitoring has induced a demand for automated analytical systems with sensitive sensors. Such sensors have to fulfil requirements such as reliability, low cost, low power consumption, small sample volumes, adaptation to fluidic systems, and autonomous operation capability. To achieve this, sensors with the use of light emitting diodes (LEDs) as light sources and sensing devices with LEDs for excitation and detection of absorption and fluorescence according to the paired-emitter-detector-diode (PEDD) concept have been demonstrated for environmental monitoring [6,7].

Fluorescence detectors based on free beams for capillary electrophoresis have been implemented using LEDs as light sources and photodiode [8] or photomultiplier tube [9] as detectors. In both types excitation and emitted light were created by diffractive and dispersive elements such as lenses or objectives.

The use of liquid core waveguides (LCW) for environmental analysis has significantly increased in the last decade [10]. Such light guiding capillaries can be used for sensitive absorption spectrophotometry by the increased light–matter interaction, i.e.

* Corresponding author. Tel.: +49 3641206278; fax: +49 3641206299.
E-mail address: lars.kroeckel@ipht-jena.de (L. Kröckel).

http://dx.doi.org/10.1016/j.talanta.2014.02.072
0039-9140

increased interacting length [10]. Furthermore, these waveguides are currently being used for the detection of chemiluminescence and photoluminescence [11]. For luminescence applications the substance to be analysed is transversally illuminated and the emitted light is then guided through the LCW coupled into an optical fibre and finally detected via a photodiode [11,12], a photomultiplier tube [11], or a CCD array spectrometer [13]. Dasgupta et al. [14] demonstrate a LCW sensor with a transversally fibre coupled LED for excitation. LCWs are commercially available as flexible silica capillary with an outer Teflon® AF Fluoro-polymer coating (Polymicro technologies) or as pure Teflon® AF capillaries (Biogeneral Inc.).

In the present work we report on a new concept of a miniaturised fluorescence detector. The device is compact and is designed for flow analysis. Its main features are large collection of the isotropically emitted light, strong suppression of the exciting light and low consumption of sample and reagents volumes. To reveal its performance we chose to detect orthophosphate in water.

The spectrophotometric determination of soluble reactive phosphorus by flow injection analysis (FIA) based on determining the formation of molybdophosphate heteropoly acid has been widely studied [10,15–21]. Unfortunately, the spectrophotometric method is inherently slow. The time response could be shortened by increasing the operation temperature which, inappropriately, would result in a higher demand of equipment, energy, and space. Another sensitive spectrophotometric method for FIA application relies on the formation of an ion-association complex of molybdophosphate with Malachite Green [22,23]. This method is extensive and time-consuming due to the collection and concentration via a tiny membrane filter and solving the ion associate in methyl cellosolve. Another useful method for determining phosphate is a fluorimetric method which monitors the fluorescence of thiochrome, formed by the oxidation of thiamine by heteropoly acid [24,25]. However, because of the high cross-sensitivity towards both Fe(III)- and Cu(II)-ions this fluorimetric method is not suitable for seawater measurements. To avoid all mentioned difficulties we choose another fluorimetric method for the determination of trace amounts of phosphate in water and seawater. The determination of free reactive phosphorus is based on the reaction of phosphate with molybdate ions to phosphomolybdate which quenches the fluorescence of Rhodamine 6G [26–33]. This chemical method is well established and has found application in various field such as FIA [20–22,25], SIA (sequential injection analysis) [26,27], flotation-fluorophotometry [23], membrane filtration [24], or is used for online preconcentration [25].

Furthermore, a fast reversed flow injection analysis (R-FIA) system with a new concept of pressure decoupling for fast in situ applications (for example: integration of the R-FIA system in an undulating towed vehicle) has additionally been developed. The fluorescence detector was integrated into the R-FIA system and tested with pure water and synthetic seawater under lab conditions.

2. Material and methods

2.1. Applied chemical method and reagents

Our employed method is based on the reaction of orthophosphate with molybdate under acidic conditions producing molybdophosphate, a chemical forming a non-fluorescent complex with Rhodamine 6G [26–33].

In our system this reaction leads to a decrease in the fluorescence intensity by a static fluorescence quenching. This quenching-concentration dependency is described by the Stern–Volmer relationship [34],

$$\frac{I_0}{I} = 1 + K_s\, Q \tag{1}$$

with I_0 and I being the intensities of fluorescence without and with a quencher, respectively, the Stern–Volmer quenching constant K_S and the quencher concentration Q.

A linear behaviour (see Supplementary material, Fig. S1, $I_0/I = 1 + 0.004 \times 10^6\ \mathrm{L\,g^{-1}}\ (PO_4\text{–}P)\ [Q]$) was achieved when mixing 1 mL RS1, 1 mL RS2 and 1 mL of phosphate standard solutions in a 1 cm cuvette (the excitation wavelength was 470 nm).

All the reagents employed were of analytical grade (Merck or Sigma-Aldrich) and all solutions were prepared with ultrapure water (conductivity 0.055 μS cm^{-1}, Siemens Water Technologies). Synthetic seawater and ultrapure water were utilised as the carrier and sample. Our phosphate working standards were daily prepared from a commercial 326.12 mg L^{-1} PO_4–P stock solution (Merck). For seawater experiments, phosphate standards were freshly prepared in a seawater standard solution (according to [35], salinity measured to 29.55). The composition of the synthetic seawater is listed in Supplementary material Table S1.

Viscosity measurements of the carrier solutions were performed using Hoeppler viscosimeter.

Reagent solution 1 (RS1) and reagent solution 2 (RS2) were derived from [22]. The reagent solution 1 consists of Rhodamine 6G (1.5 mg L^{-1}) and the emulsifier p-octylphenoxypolyethoxyethanol (500 mg L^{-1}). Rhodamine stock solution (250 mg L^{-1}) was made by dissolving 25 mg in 100 mL water. To prepare RS1 1.5 mL Rhodamine stock solution was added to 100 mL water. 2.5 mL of 5% emulsifier was added and the solution was diluted to 250 mL. The reagent solution 2 is made up of molybdate (58 mmol L^{-1}), hydrochloric acid (1 mol L^{-1}), and also p-octylphenoxypolyethoxyethanol (500 mg L^{-1}). To prepare RS2 1.024 g ammonium heptamolybdate was solved in 50 mL hydrochloric acid (1 mol L^{-1}) in a 100 mL flask. We added 1 mL 5% emulsifier and fill it up to the calibration mark with hydrochloric acid (1 mol L^{-1}). All solutions were filtered, degassed and stored in plastic bottles [36].

2.2. Optical detector for fluorescence measurements

Fluorescence detectors for online applications in water must fulfil specific requirements, which are: small spatial footprint, small sample volume, adaptation to the fluidic system, high attenuation of the exciting light, and effective collecting of the diffusely emitted fluorescence.

The functional principle of our fluorescence detector relies on the phosphate-induced fluorescence quenching of the dye Rhodamine 6G with higher phosphate concentration leading to a more quenched fluorescence. Rhodamine 6G has maximum absorption and fluorescence at 527 nm and at 556 nm, respectively (Fig. 1). For fluorescence excitation a blue LED (product no. 5B4HCA-H, Roithner Lasertechnik GmbH, diameter 5 mm, stable current 10.6 mA) with an emission peak at 470 nm and full-width-half-maximum (FWHM) of 25 nm was used. For suppressing the exciting light an edge filter (OG 530, Schott AG) was used. Only 0.3% of the LED light passes through the filter.

The detector (Fig. 2(a)) was made of a black cubic-formed capillary holder (material: polyoxymethylene) with a central hole for the borosilicate glass capillary (outer diameter: 3 mm, inner diameter: 1 mm, both ends of the capillary were polished under an angle of 21° for the fluid inlet). The holder has four openings, one at each side around the capillary, which are reduced at an angle of 31°, leading to a 1 mm thick and 6 mm long open detection channel to the capillary. The detection volume is 4.7 μL. The fluorescence inside the capillary is excited via a multimode fibre (mmF) which is stuck into the capillary, with its end being

precisely positioned close to the location of the actual detector unit. The mmF is connected to the blue LED. Strong light transfer from LED into glass capillary is ensured by using a 550 μm thick mmF (All Silica Low OH 550, Laser Components GmbH) with a numerical aperture of 0.22. The fibre ends outside the detection channel of the capillary holder. The fluorescence light is collected by a photodiode (KOM 2125, Siemens AG) using by a high-aperture converging lens (NA=0.51, it is made of two paired Fresnel lenses glued together). Undesired excitation light is suppressed via an edge filter positioned in front of the photo detector. For FIA applications the detector is equipped with appropriate fluidic adaptors.

The developed fluorescence detector has a dynamic measuring range of 19.6 dB, showing a linear response up to 750 $\mu g\,L^{-1}$ Rhodamine 6G with a slope of 0.01 $V\,L\,\mu g^{-1}$ and a lowest detectable concentration of 1 $\mu g\,L^{-1}$ (2.09 $nmol\,L^{-1}$). For the concentration range up to 750 $\mu g\,L^{-1}$ a maximum absorbance of 0.02 is reached.

2.3. FIA arrangement

Reversed-FIA is based on injecting the reagents into a sample stream used as carriers. This method is applied when sample material is abundant and is characterised by low reagent consumption and high sample throughput [37–39].

Our developed R-FIA setup (Fig. 2(b)) for measuring phosphate is composed of two main parts: sample acquisition and sample analysing. The arrangement of the analytical setup consists of a reagent container, a mixing coil and the developed fluorescence detector. A higher sensitivity with respect to the analysis of nutrients was obtained by an in-house developed fluid mixer which was integrated in the analysing part.

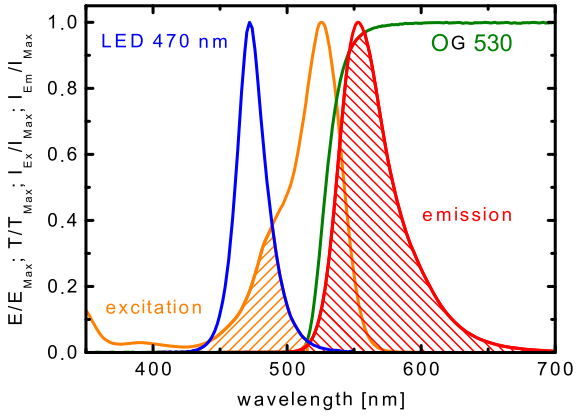

Fig. 1. Normalised fluorescence excitation and emission of Rhodamine 6G, emission spectra of chosen LED and transmission curve of edge filter OG 530; E – extinction, T – transmission, I_{ex} – intensity of excitation light, I_{em} – intensity of emission light.

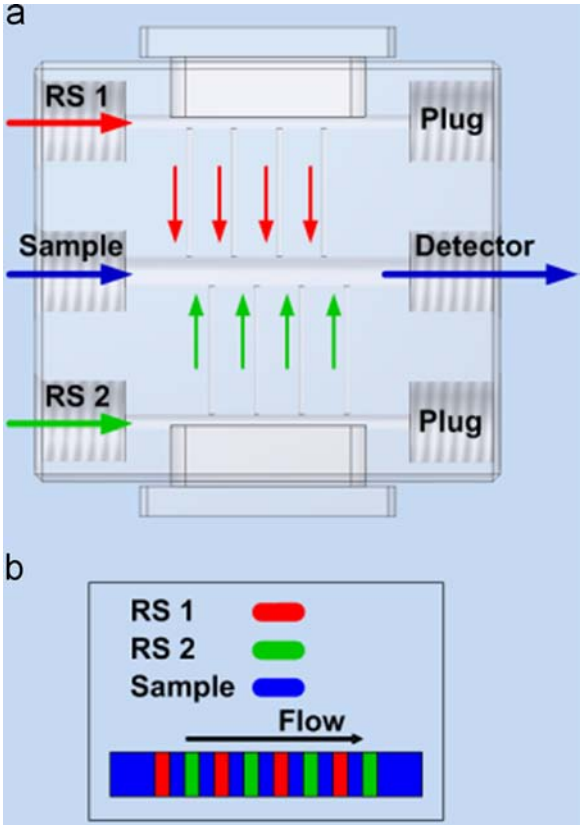

Fig. 3. (a) Schematic of the mixer and fluidic connections. (b) Injection sequence of sample and reagents. The mixer is made of polycarbonate.

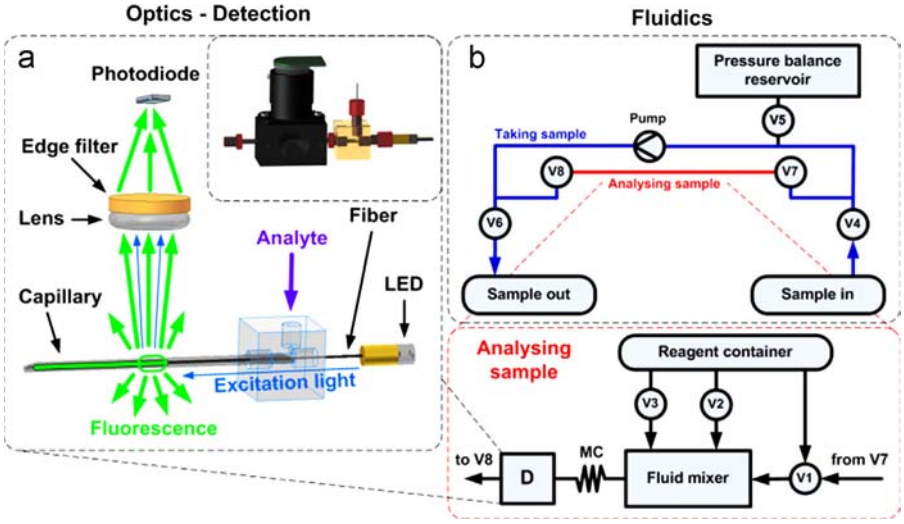

Fig. 2. (a) Sketch of the developed fluorescence detector with optical components. In the upper right corner the 3D model of the fluorescence detector is shown. (b) Constructed R-FIA system with acquisition unit and analysis part; Pump: mzr-4605 (HNP Mikrosysteme GmbH); MC: mixing coil (75 cm, ID: 0.75 mm); valves: V1-V3: 3/2-way 161T031 (NResearch Inc.), V1 – standard, V2 – RS2, V3 – RS1, V4–V8: 2/2-way rocker solenoid valves (Christian Bürkert GmbH & Co. KG); D: detector.

The R-FIA technique we used here is based on a repeating sequence of sample and reagent injections yielding a maximum sensitivity. Accordingly our mixer generates a sequence of samples and reagents injected at four injection points (mixer is shown in Fig. 3(a)). The four injection channels (diameter: 0.2 mm, distance between each channel: 3 mm) on each side are connected via a channel, 19 mm long and 2 mm in diameter. The injection procedure consists of four steps (Fig. 3(b)): during the first step of the analysing process the sample flows through the middle channel of the mixer and the analysing part of the system is rinsed. Then the flow stops and the reagents are consecutively injected, first RS2 then RS1. To obtain a better radial mixing and to achieve a nearly Gaussian-shaped, but unsymmetrical, measuring signal (inset Fig. 5), a meander formed reaction tube with a channel length of 75 cm (inner diameter: 0.75 mm) followed the fluid mixer. Our setup provides sufficient mixing of reagents and sample on the way to the detector unit.

3/2-way isolation valves V1, V2 and V3 (161T031, NResearch Inc., Fig. 3(b)) are used for injecting the reagents (RS2 and RS1) and for an external standard as quality control. These valves can handle only a maximum pressure difference of 2 bars, but are able to inject small volumes with a very high repeatability. Variation coefficients of 1% and 0.6% for injection volumes of 15 μL and 50 μL at 50 measurements were calculated by weighing the volumes, respectively. Infusion bags filled with the reagents and the calibration standard are put into the reagent container. With a volume of 100 mL approximately 6000 measurements for an injected volume of 15 μL can be performed. The dosing of the reagents occurs at a constant pressure difference of 500 mbar ± 1% between the reagent container and the ambient pressure of the R-FIA system. For the generation of the pressure difference a small membrane pump (SP 600-EC-LC 12 V dc, Schwarzer Precison GmbH & Co., KG) is used and the pressure difference is controlled by a differential pressure regulator (BSW001DV-PCB, Sensortechnics GmbH).

The sample taking part is built up with a valve manifold and a micro annular gear pump (mzr-4605, HNP Mikrosysteme GmbH), which protect the analytical part from the environmental pressure. The five valves (V4-V8) on the valve manifold (see Supplementary material Fig. S2) are 2/2-way rocker solenoid valves (6608, Christian Bürkert GmbH & Co., KG), which are normally closed and designed for a pressure difference of 10 bar (they can work against 14 bar when small modification are implemented). All used tubing is made from PTFE and has inner diameters of 1.0 mm unless otherwise stated.

Undesired particles in the sample may influence the flow inside the fluidic system and could potentially lead to plugging.

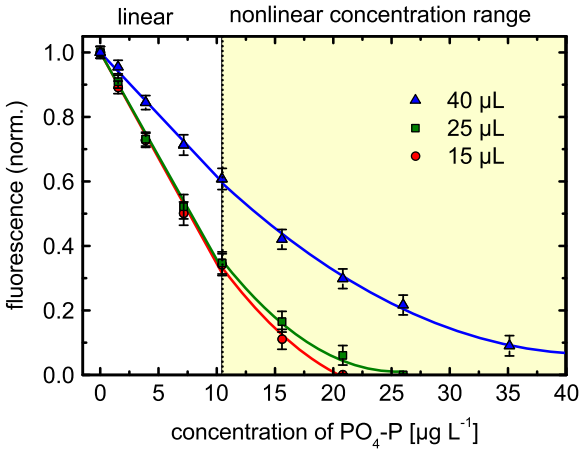

Fig. 4. Fluorescence-concentration dependency for three injection volumes at a constant flow velocity of 4.3 mL min^{-1} and a reaction tube length of 75 cm (linear regime: white and nonlinear regime: yellow). Error bars ± 3 standard deviation, n=15. (For interpretation of the references to colour in this figure legend, the reader is referred to the web version of this article.)

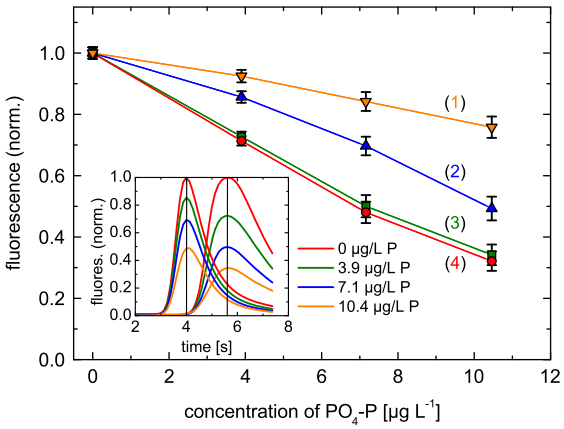

Fig. 5. Fluorescence signals versus phosphate concentration for different flow velocities (7.1 (1), 6.1 (2), 4.3 (3) and 3.5 (4) mL min^{-1}) at constant injected volumes of 15 μL. Inset: original measurement data of the flow rate experiments for 4.3 and 6.1 mL min^{-1} are shown. Error bars ± 3 standard deviation, n=15.

Furthermore, particles can induce disturbing scattering of light in every measurement. To avoid such negative impacts samples ought to be filtered prior to the actual measurements. For online applications a cross-flow filter (pore size: 0.2 μm) could be installed in front of V4. A major advantage of our system is that it requires only small volumes, allowing to use the filter for long times.

The measurement procedure begins by pumping the sample continuously through the sample taking circuit (V4 and V6 are open). The flow is then stopped, V4 and V6 are closed. The pressure inside the sample taking part is balanced by a short opening of valve V5. Subsequently the valves V7 and V8 are opened and the analysing circuit is rinsed with the fresh sample. Then the flow is stopped again and the reagents, RS2 and RS1, are injected via valves V2 and V3 into the fluid mixer and, consequently, into the sample as well. During the injection the valve V5 stays open. The pump is switched on again and the three compounds are then mixed in the fluid mixer and in the meander reaction tube. The fluorescence quenching that results from the reaction is measured by the fluorescence detector. A DIMM-PC (DIMM – Dual inline memory module, -4H-Jena engineering GmbH) controls the fluidic systems, runs and evaluates the measurements. The flow rate is regulated by the revolution speed of the pump and can be adjusted between 0.012 and 72 mL min^{-1}. Different flow rates are used for the several processes during the analysis. The dead volume of the R-FIA system is 4.1 mL, at which the analysing part has a volume of 570 μL. The volume of the sample acquisition part is nearly six times higher, which is sufficient to rinse the analysing part and to fill it with an uncontaminated sample.

Rinsing the entire fluidic system for five minutes with ultrapure water after usage is sufficient for cleaning. In case of a shut-down period the water inside the system should be removed by flushing with dried nitrogen.

For lab analysis the sample taking part is not necessary, so the fluid system can be simplified and one measurement needs only 12 s, corresponding to a sampling rate of 300 measurements per hour. For in situ applications the sample taking circuit has to be added and consequently one measurement takes 20 s resulting in a sampling rate of 180 measurements per hour.

3. Results and discussion

3.1. Influence of reagents concentrations

The influence of the reagent's concentrations on the determination of phosphate was studied by varying the concentration of

Rhodamine 6G, molybdate, hydrochloric acid and emulsifier. The optimisation of the reaction was carried out using the R-FIA setup under constant fluidic parameters: mixing coil length 50 cm, flow velocity 4.3 mL min^{-1}, reagents injection volumes 50 μL.

First the concentration of Rhodamine 6G was varied in the range of 1.5–5 mg L^{-1} (see Supplementary material Fig. S3(a)). The fluorescence intensity falls and, therefore the sensitivity increases by decreasing the Rhodamine 6G concentration. The number of formed molybdophosphate and consequently the number of non-fluorescent complexes are kept constant under unchanged conditions, leading to a rise in fluorescence intensity by increasing the Rhodamine 6G concentrations. To achieve a high sensitivity over a wide phosphate concentration range we choose a Rhodamine 6G concentration of 1.5 mg L^{-1}. The sensitivity is given by the slope of the normalised fluorescence dependency on phosphate concentration, where the maximum fluorescence signals (inset Fig. 5) are normalised to the maximum peak of the fluorescence signal of the blank value (RS1+RS2 without phosphate).

In the next step the concentration of molybdate was studied in the range of 0.014–0.073 mol L^{-1}. The fluorescence intensity declines by increasing the molybdate concentration up to 0.058 mol L^{-1} (see Supplementary material Fig. S3(b)). Beyond this concentration there was no change in observed signals. Hence, a 0.058 mol L^{-1} molybdate concentration was used in subsequent work.

The emulsifier was added to both reagent solutions, RS1 and RS2, to reach a homogenous distribution of the dissolved reactants and to improve the reproducibility of the phosphate determination. Another role of the emulsifier is to prevent the deposition of Rhodamine 6G and the formed complexes on the inner tubing wall. Concentrations of 0, 0.5, 2.5 and 5 g L^{-1} emulsifier in both reagent solutions were tested. The two highest concentrations lead to the formation of undesired air bubbles. Without emulsifier the repeatability of the measuring signals was poor. Finally an emulsifier concentration of 0.5 g L^{-1} was chosen for both reagent solutions.

In the next step the concentration of hydrochloric acid in RS2 was varied in the range between 0.25 and 4 mol L^{-1}. The sensitivity reached a maximum for 1 mol L^{-1} hydrochloric acid, which was used in all further discussed experiments.

3.2. Influence of fluidic parameters

The selection of the fluidic parameters influences the residence time of the reagents, and therefore, the reaction time, sensitivity and sampling rate. We investigated the influence of injected volumes of reagents, reaction tube length, and flow velocity in order to maximise the sensitivity and sample frequency, and reduce reagent consumption.

For applications to seawater measurements a high sensitivity is desirable to fit the requirements of the existing nutrient. For instance, the phosphate concentrations at the surface in the German Bight (North Sea) ranges from 0.36 to 0.89 μmol L^{-1} PO_4–P (11.15–27.56 μg L^{-1} PO_4–P) and increased to 1.71 μmol L^{-1} PO_4–P (53 μg L^{-1} PO_4–P) at the Elbe estuary [40]. In the Baltic Sea phosphate concentrations were measured down to 0.03 μmol L^{-1} PO_4–P (0.93 μg L^{-1} PO_4–P) [40]. To achieve such high sensitivities and low LOD's we developed the fluid mixer described in Section 2.3. The task of the mixer is to efficiently premix the three components (RS1, RS2 and sample).

To investigate the influence of the injected volume into the fluid mixer, 15 μL, 25 μL or 40 μL of each reagent were injected into the sample stream (Fig. 4). A linear relationship is only found up to a phosphate concentration of approximately 10 μg L^{-1} PO_4–P. Higher concentrations require a nonlinear fitting function. The linear and nonlinear calibration functions are listed in Table 1. Increasing the injection volume of reagents from 15 μL to 40 μL reduces the sensitivity of the linear part from 0.066 L $μg^{-1}$ PO_4–P to 0.038 L $μg^{-1}$ PO_4–P. No significant sensitivity difference between injected volumes of 15 μL and 25 μL is observed (correlation coefficient for all linear calibration curves is 0.999).

The results indicate that the measurement range and the sensitivity can be adjusted precisely by the injected volume of reagents. So with an injection volume of 40 μL concentrations up to 40 μg L^{-1} can be determined by the quadratic function $y = -0.044\ L\ \mu g^{-1}\ (PO_4\text{–}P)\ x + 5.4 \times 10^{-2}\ L^2\ \mu g^{-2}\ (PO_4\text{–}P)\ x^2 + 1$ (for pure water, $R^2 = 0.999$). Nearly twice the sensitivity is obtained with an injection volume of 15 μL and concentrations up to 15 μg L^{-1} can be determined by the quadratic function $y = -0.079\ L\ \mu g^{-1}\ (PO_4\text{–}P)\ x + 1.5 \times 10^{-3}\ L^2 \mu g^{-2}\ (PO_4\text{–}P)\ x^2 + 1$ (for pure water, $R^2 = 0.999$).

An additional investigation revealed that the injection sequence plays a significant role leading to a 1.5 times higher sensitivity when RS2 is first injected.

The effect of reaction tube length was studied with 25, 50, 75 and 100 cm. Although higher sensitivity was achieved with the 100 cm tube length, the 75 cm was chosen since it presented a better repeatability due to lower dispersion and weaker peak broadening. Regarding the configuration of the reaction tube a better radial mixing and a nearly Gaussian-shaped, but unsymmetrical, measurement signal was obtained when a meander formed tube was used (inset, Fig. 5).

The influence of the flow velocity has been investigated with four different flow rates: 3.5, 4.3, 6.1 and 7.1 mL min^{-1} (Fig. 5 inset shows exemplarily the original fluorescence signals for the flow rates of 4.3 and 6.1 mL min^{-1}).

The increase of the sensitivity at lower flow velocities results from the change of the reagents dispersion and from the higher residence time of the reagents in the system. The lower flow rate allows the analytical compounds to have more time to react with each other and consequently lead to a larger fluorescence quenching. Below a flow rate of 4.3 mL min^{-1} there was no significant change in sensitivity. Hence, this flow rate was therefore chosen, considering sensitivity and sample frequency.

3.3. Influence of salinity

For seawater applications the effect of changes in the salinity was investigated. First the influence of sodium chloride (NaCl) on the blank value (RS1+RS2 without phosphate) in the range between 0 and 40 g L^{-1} was studied (NaCl has no influence on the analytic reaction [28]). Then, in a next step, NaCl was replaced by artificial seawater (salinity between 0 and 40) and the setup was investigated in the same way. A decrease of the fluorescence signal by increasing the concentrations of sodium chloride and synthetic

Table 1
Calibration functions for three injection volumes.

Injection volume [μL]	Linear concentration range	Nonlinear concentration range
40	$y = -0.038\ L\ \mu g^{-1}\ (PO_4\text{–}P)\ x + 1$	$y = -0.044\ L\ \mu g^{-1}\ (PO_4\text{–}P)\ x + 5.4 \times 10^{-2}\ L^2\ \mu g^{-2}\ (PO_4\text{–}P)\ x^2 + 1$
25	$y = -0.064\ L\ \mu g^{-1}\ (PO_4\text{–}P)\ x + 1$	$y = -0.077\ L\ \mu g^{-1}\ (PO_4\text{–}P)\ x + 1.5 \times 10^{-3}\ L^2\ \mu g^{-2}\ (PO_4\text{–}P)\ x^2 + 1$
15	$y = -0.066\ L\ \mu g^{-1}\ (PO_4\text{–}P)\ x + 1$	$y = -0.079\ L\ \mu g^{-1}\ (PO_4\text{–}P)\ x + 1.5 \times 10^{-3}\ L^2\ \mu g^{-2}\ (PO_4\text{–}P)\ x^2 + 1$

seawater was observed (see Supplementary material Fig. S4). The two similarly decreasing curves can be fitted by one linear function given by $y=-6.23\times10^{-3}x+1$ ($R^2=0.999$). By increasing the concentrations of NaCl and the salinity of artificial seawater the fluorescence signal curves started later and were broadened so that the peaks of the recorded graphs were shifted up to one second and consequently fell. Assuming no induced fluorescence quenching the delayed fluorescence signal is explained by a change of viscosity: we measured the two viscosities at a constant temperature of 25.6 °C, giving 0.888…0.977 mPa s for NaCl and 0.888…0.983 mPa s for artificial seawater. These two viscosities lead to different injection volumes of reagents and can be compensated by increasing the opening times of the injection valves and the measurement of the salinity.

It is reported that silicate ions have a significant influence on the phosphate determination. However, the reaction of phosphomolybdate and Rhodamine 6G relevant here is not influenced by this ion, and thus an influence of silicate on our results is not investigated further [29,30].

For phosphate analyses in synthetic seawater a linear calibration curve over the range 0–10 μg L^{-1} PO_4–P was obtained ($y=-0.044$ L μg^{-1} (PO_4–P) $x+1$, $R^2=0.996$) and with a nonlinear calibration curve given by $y=-0.052$ L μg^{-1} (PO_4–P) $x+6.8\times10^{-4}$ L^2 μg^{-2} (PO_4–P) x^2+1 with a correlation coefficient of 0.999 concentrations up to 40 μg L^{-1} PO_4–P can be determined.

3.4. Analytical figures of merit

Using the optimised parameters (Table 2) calibration curves for pure water and synthetic seawater in a phosphate concentration range between 0 and 40 μg L^{-1} PO_4–P were obtained. For both matrices linear regression functions with highest achieved sensitivities for reagents injection volumes of 15 μL can be applied to concentrations up to 10 μg L^{-1} PO_4–P. Using three times the standard deviation of the blank value divided by the slope of the linear calibration graph [41], we calculated the LODs of 0.22 μg L^{-1} PO_4–P (7 nmol L^{-1}) for pure water and of 0.45 μg L^{-1} PO_4–P (14.5 nmol L^{-1}) for seawater, respectively. Using quadratic calibration functions for injected reagents volumes of 40 μL phosphate levels up to 40 μg L^{-1} can be determined precisely.

The repeatability of the R-FIA system was assessed by the determination of the relative standard deviation (RSD) values of eighteen measurements series with the following sequence: blank value, 3.9 μg L^{-1} PO_4–P, 7.1 μg L^{-1} PO_4–P, 10.4 μg L^{-1} PO_4–P, 20.8 μg L^{-1} PO_4–P and again blank value – fifteen single measurements for each solution were taken in one series. The achieved relative standard deviations are between 0.6% for the blank value signal and 4.6% for a phosphate concentration of 20.8 μg L^{-1} PO_4–P. Furthermore, the R-FIA system was tested to work against a pressure difference of 6 bar showing that the measurements were not influenced.

The R-FIA system together with the developed fluorescence detector described here has an improved or at least similar performance for online phosphate determination compared to other reported in literature. Frank et al. [32,33] reported on a sequential injection analysis (SIA) system for the determination of phosphate for coastal water monitoring using the same analytical reaction used here. They show a detection limit of 50 nmol L^{-1} and a sampling rate up to 270 measurements per hour. Motomizu et al. [42] achieved a LOD of 10 nmol L^{-1} and the sampling rate was 15 samples per hour by substituting Rhodamine 6G by Rhodamine B. The use of liquid waveguide capillary cells (LWCC) for the spectrophotometric detection of phosphate, based on the formation of the blue form of reduced phosphomolybdate (molybdenum blue), has increased in the last decade, yielding LODs in the range between 0.5 nmol L^{-1} and 10 nmol L^{-1} [10,15–21]. To achieve such low detection limits LWCC lengths of up to 250 cm are necessary, which in fact can lead to air or micro-bubble formation at the large internal surface of the waveguide, reducing the reliability of the measurements [10,17].

Table 2
Optimised parameters for the R-FIA system discussed here.

Parameter	Selected value
Injection volume into fluid mixer (μL)	15, 40
Measuring range (μg L^{-1})	0–15, 0–40
Length of mixing coil (cm)	75
Flow rate (mL min^{-1})	4.3
Rhodamine 6G concentration (mg L^{-1})	1.5
Molybdate concentration (mol L^{-1})	0.058
Emulsifier concentration (g L^{-1})	0.5

4. Conclusions

A miniaturised, robust and low-cost fluorescence detector for FIA applications is presented. It reveals an excellent sensitivity and is highly selective to the chosen analyte. The concept of our flow-through sensor is demonstrated using the reaction of phosphate with molybdate producing molybdophosphate, which quenches the fluorescence of Rhodamine 6G. The straightforward design of the presented fluorescence sensor seems to be applicable for the development of similar flow-through detectors for the determination of many other fluorescent species or analytic reactions. Further developments will concentrate on improving the fluorescence detector to gain more spectral information. For instance, sensitive fluorescence and absorption measurements [43] could be combined in one device. Moreover we are planning to replace the photodiode by a miniaturised spectrometer (MINOS, IPHT) to make our device commercially more interesting.

Additionally, an R-FIA concept was established relying on pressure decoupling for in situ applications. Exhibiting the high speeds, low reagent (15 μL per sample) consumptions, high sensitivity (LODs of 0.22 μg L^{-1} PO_4–P (7 nmol L^{-1}) for pure water and of 0.45 μg L^{-1} PO_4–P (14.5 nmol L^{-1}) for seawater) and a significant mechanical robustness this setup has the capability to be applicable for surface or underway monitoring of phosphate in seawater. Compared to other published concepts the developed fluorimetric sensor and the R-FIA system together have a better or equal performance in terms of sensitivity, detection limits and sampling rate. The use of our system in laboratories is possible, in which case the fluidic setup can be simplified by only using the analytical part. The developed R-FIA system is very flexible, as it can be adjusted to suit any other chemical analytical reactions.

Acknowledgement

This work was funded by the German Federal Ministry of Education and Research (Project no. 03F0365C) and by the Thuringian State Ministry for Economics, Labour and Technology (Project no. 2012FGR0013) supported by the European Social Funds (ESF).

Appendix A. Supplementary material

Supplementary data associated with this article can be found in the online version at http://dx.doi.org/10.1016/j.talanta.2014.02.072.

References

[1] I.D. McKelvie, S.D. Kolev, P.J. Worsfold, Pure Appl. Chem. 84 (2012) 1973–1982.
[2] G. Mills, G. Fones, Sens. Rev. 32 (2012) 17–28.
[3] A. Morales-Rubio, M. de la Guardia, B.F. Reis, Trends Anal. Chem. 28 (2009) 903–913.
[4] P. Loewe, H. Klein, G. Becker, H. Nies, U. Brockmann, S. Schmolke, S. Dick, D. Schrader, A. Frohse, A. Schulz, J. Herrmann, N. Theobald, B. Klein, S. Weigelt, Condition of the North Sea 2004, Bundesamt für Seeschifffahrt und Hydrographie, Hamburg and Rostock, 2006.
[5] S. Gray, G. Hanrahan, I. McKelvie, A. Tappin, F. Tse, P. Worsfold, Environ. Chem. 3 (2006) 3–18.
[6] M. O'Toole, D. Diamond, Sensors 8 (2008) 2453–2479.
[7] L. Tymecki, M. Rejnis, M. Pokrzywnicka, K. Strzelak, R. Koncki, Anal. Chim. Acta 721 (2012) 92–96.
[8] F.-B. Yang, J.-Z. Pan, T. Zhang, Q. Fang, Talanta 78 (2009) 1155–1158.
[9] B. Yang, F. Tan, Y. Guan, Talanta 65 (2005) 1303–1306.
[10] M.D. Patey, M.J.A. Rijkenberg, P.J. Statham, M.C. Stinchcombe, E.P. Achterberg, M. Mowlem, Trends Anal. Chem. 27 (2008) 169–182.
[11] P.K. Dasgupta, Z. Genfa, J. Li, C.B. Boring, S. Jambunathan, R. Al-Horr, Anal. Chem. 71 (1999) 1400–1407.
[12] J. Li, P.K. Dasgupta, Z. Genfa, Talanta 50 (1999) 617–623.
[13] R.H. Byrne, W. Yao, E. Kaltenbacher, R.D. Waterbury, Talanta 50 (2000) 1307–1312.
[14] G. Song, I. Villanueva-Fierro, S.-I. Ohira, S. Mishra, H. Bailiff, C.R. Savage, P.K. Dasgupta, Talanta 77 (2008) 901–908.
[15] J.Z. Zhang, J. Chi, Environ. Sci. Technol. 36 (2002) 1048–1053.
[16] L.J. Gimbert, P.M. Haygarth, P.J. Worsfold, Talanta 71 (2007) 1624–1628.
[17] L.A. Zimmer, G.A. Cutter, Limnol. Oceanogr. Methods 10 (2012) 568–580.
[18] J. Ma, D. Yuan, M. Zhang, Y. Liang, Talanta 78 (2009) 315–320.
[19] Q.P. Li, D.A. Hansell, J.-Z. Zhang, Limnol. Oceanogr. Methods 6 (2008) 319–326.
[20] M.D. Patey, E.P. Achterberg, M.J.A. Rijkenberg, P.J. Statham, M. Mowlem, Anal. Chim. Acta 673 (2010) 109–116.
[21] M.D. Krom, E.M.S. Woodward, B. Herut, N. Kress, P. Carbo, R.F.C. Mantoura, G. Spyres, T.F. Thingstand, P. Wassmann, C. Wexels-Riser, V. Kitidis, C.S. Law, G. Zodiatis, Deep-Sea Res. II 52 (2005) 2879–2896.
[22] S. Motomizu, T. Wakimoto, K. Toei, Talanta 30 (1983) 333–338.
[23] S. Motomizu, T. Wakimoto, K. Toei, Analyst 108 (1983) 361–367.
[24] T. Pérez-Ruiz, C. Martínez-Lozano, V. Tomás, J. Martín, Anal. Chim. Acta 442 (2001) 147–153.
[25] B. Zhang, H.P. Beck, Anal. Lett. 34 (2001) 2721–2733.
[26] S. Motomizu, H. Mikasa, M. Oshima, K. Toei, Bunseki Kagaku 33 (1984) 116–119.
[27] S. Zitai, Q. Wenqi, C. Shuyu, L. Shuqin, Environ. Chem. 7 (1988) 45–48.
[28] W. Fusheng, W. Zhongxiang, T. Enjiang, Anal. Lett. 22 (15) (1989) 3081–3090.
[29] M. Taga, M. Kann, T. Nasu, Z. Fresenius, Anal. Chem. 334 (1989) 45–48.
[30] M. Kan, T. Nasu, M. Taga, Anal. Sci. 7 (1991) 87–91.
[31] T. Taniai, M. Sukegawa, A. Sakuragawa, A. Uzawa, Talanta 61 (2003) 905–912.
[32] C. Frank, F. Schroeder, R. Ebinghaus, W. Ruck, Talanta 70 (2006) 513–517.
[33] C. Frank, F. Schroeder, R. Ebinghaus, W. Ruck, Microchim. Acta 154 (2006) 31–34.
[34] L.K. Frakjii, D.M. Hayes, T.C. Werner, J. Chem. Educ. 69 (1992) 424–428.
[35] J.I. Drever, The Geochemistry of Natural Waters, Third Edition. Prentice-Hall, Upper Saddle River, N.J., 1997, p. 436.
[36] J.-Z. Zhang, C.J. Fisher, P.B. Ortner, Water Res. 33 (1999) 2879–2882.
[37] J. Ruzicka, E.H. Hansen, Flow Injection Analysis, second ed., Wiley, New York, 1988.
[38] J. Ruzicka, E.H. Hansen, Anal. Chim. Acta 99 (1978) 37–76.
[39] J. Ruzicka, E.H. Hansen, Anal. Chim. Acta 145 (1983) 1–15.
[40] ⟨http://www.bsh.de/de/Meeresdaten/Beobachtungen/MURSYS-Umweltreport system/updates.jsp⟩ (29/11/13).
[41] J.C. Miller, J.N. Miller, Statistics for analytical chemistry, third ed., Ellis Hollywood Ltd., Chichester, UK, 1993.
[42] S. Motomizu, M. Oshima, N. Katsumura, Anal. Sci. Technol. 8 (1995) 843–848.
[43] L. Kröckel, G. Schwotzer, H. Lehmann, T. Wieduwilt, Water Res. 45 (2011) 1423–1431.